Review of Scientific Instruments ARTICLE scitation.org/journal/rsi

Lock-in frequency measurement with high precision and efficiency

Cite as: Rev. Sci. Instrum. 91, 075106 (2020); doi: 10.1063/5.0002377
Submitted: 24 January 2020 • Accepted: 23 June 2020 •
Published Online: 7 July 2020

Jun Lu (陆俊)[a]

AFFILIATIONS

Institute of Physics, Chinese Academy of Sciences, Beijing National Laboratory for Condensed Matter Physics, Beijing 100190, China

[a]Author to whom correspondence should be addressed: lujun@iphy.ac.cn

ABSTRACT

This paper describes a new method of frequency measurement based on lock-in amplifiers (LIAs). In contrast to other frequency measurement methods, such as fast Fourier transformation (FFT), zero crossing, and scanning autocorrelation, this method is based on an adaptable LIA design for high-precision determination of not only the frequency but also the amplitude and phase of periodic signals, even when they are buried in heavy noise with low signal-to-noise ratios. Mathematical derivation of the local spectrum around the center frequency is performed, and the local frequency spectrum waveform of the sinusoidal signal, regardless of whether it is pure or noisy, is found to be exactly of a bell shape that can be described by a three-parameter sine function. Based on the principle of LIAs, the correct frequency can produce a peak amplitude in the local spectrum. As a result, the amplitudes of three frequency points around the target frequency can be used to precisely determine the peak frequency via sinusoidal fitting. The efficiency of the proposed method is $\log_2(N)$ times that of FFT. Simulation results show that the new algorithm can reach the theoretical Cramer–Rao lower bound and remain below a lock-in upper bound. The new frequency measurement method has been implemented in an field-programmable gate array (FPGA)-based device and systematically tested for its dependence on the frequency, amplitude, and signal-to-noise ratio with typical noise types. Theoretical and experimental results show that the new method can be used in fine determination of the frequency if the user has prior knowledge of the approximate location of the frequency.

I. INTRODUCTION

Precision frequency measurements, especially for signals obscured by noise, are of great importance in many areas of scientific research and industrial applications (sound analysis, global positioning system positioning, Internet of things, and experimental physics, for example). Conventionally, three main techniques are used to measure frequency:[1,2] zero crossing, Fourier transform, and phase unwrapping. Frequency determination in terms of the number of zero crossings in one second is usually suitable for high signal-to-noise ratio (SNR) scenarios. The basic Fourier transform suffers from a finite resolution, but the discrete time Fourier transform can improve the precision at the expense of computational complexity.[3] Because phase noise obeys a white Gaussian distribution, the phase can be unwrapped and regressed to recover the frequency from a signal with a relatively low SNR.[4]

Local frequency spectrum fitting with various functions has been used to precisely determine the frequency with low computation costs,[5–10] with linear interpolation[5] and parabola fitting[6,7] being the most convenient for applications. Quinn[8] proposed a complex interpolation method using three successive Fourier coefficients with a low mean square error of the frequency estimation. Grandke[9] performed optimization tests on the pretreatment of different windows. Aboutanios and Mulgrew[10] developed iterative estimators that could converge to the true signal frequency. Boashash[11] and Jacobsen[12] reviewed and compared various frequency estimation techniques. The Cramer–Rao lower bound (CRLB) is widely used as a performance benchmark for comparing the accuracy and statistical efficiency of different estimators.[2,13,14] For estimation under various constraints, a non-Bayesian parameter estimation approach called the constrained CRLB method has also been derived.[15]

Some recent developments show that this topic continues to attract considerable interest.[16–20] Belega and Petri[16] compared two- and three-point interpolated algorithms for both complex values and modules. A novel phase estimator based on the corrected-phase

discrete Fourier transform was proposed to greatly reduce spectral leakage with a two-point joint estimation model.[17] Pulse interferences can be eliminated by an iterative algorithm.[18] Serbes[19] discussed precision frequency estimation when the phase information is already known. Remarkably, Bey proposed a highly accurate frequency estimation procedure based on multiresolution Fourier analysis and obtained vanishing variances far below the CRLB when the SNR is above the threshold value.[20]

Lock-in amplifier (LIA) measurements, previously known as phase-locking detection, involve recovering the amplitude or phase variations of an AC signal with a fixed period or frequency. This has become the most widely used method based on dynamic measurements in scientific research because of its powerful ability to detect signals buried in relatively high levels of noise or interference.[21] Traditional LIAs require prior knowledge of a signal's frequency and involve demodulators that are "locked" to the signal of interest by virtue of a synchronous or coherent reference signal. However, reference signals for LIAs are not always available with high confidence, such as in the case of misalignment due to distortion or imperfections during transmission or detection cycles. To address this problem, we propose to measure the frequency independently and with high accuracy to ensure the precision of the subsequent LIA measurements of the amplitude and phase of the periodic signal. Therefore, this measurement to be made independently from the LIA measurements is called the lock-in frequency (LIF) meter measurement.

Because LIAs function as ultranarrow bandpass filters, the LIF method is implemented after coarse estimation has been made by other methods. However, the LIF method is advantageous for accurate fine frequency determination, even in low SNR scenarios. In Sec. II, the LIF algorithm is first derived mathematically. The performance is then evaluated via simulation, after which the implementation results of the LIF instruments are given.

II. THEORY AND SIMULATION

In contrast to the fixed frequency strategy in conventional LIAs, the principle of the LIF method is to take a frequency ω as a variable and vary the virtual reference signal within a certain range. The frequency is then obtained from the maximum lock-in amplitude. Unfortunately, the precision of the frequency measurements based on the scanning LIF approach depends heavily on the scanning density, and a high scanning density naturally leads to a low efficiency. To solve this contradiction and simultaneously obtain high precision and efficiency, we analyze the results of the scanning LIF approach and find that the resulting LIF function (Δω) can be approximately considered to be a cosine function in a narrow frequency range Δω around the center frequency ω_0, as shown in Eq. (1), where the approximation in each step is based on $\Delta\omega/\omega_0 \sim 0$. This functional LIF equation was tested, the raw LIF data near the center frequency could be fitted with a sinusoidal function, and the simulation results are shown in Fig. 1, where $|\Delta\omega/\omega_0|$ is chosen below 0.7% so that the raw data cover a single functional range. The quantitative dependence of the range on the SNR and measurement condition is given in Sec. A4 of supplementary material and Sec. III. Such an adaptable LIF approach can thus be used to realize high precision frequency measurements with high efficiency under low SNR conditions. After the frequency is determined with high precision, normal LIA detection is then used to estimate the phase and amplitude at this frequency. When the amplitude of the sinusoidal signal V_p is determined, the corresponding SNR can be calculated using $\mathrm{SNR} = V_p^2/(2V_{rms}^2 - V_p^2)$, where V_{rms} is the root mean square voltage of the mixed test signal,

$$\begin{cases} LIF(\Delta\omega)_{RE} = \dfrac{2}{T_0}\displaystyle\int_0^{T_0=\frac{2\pi}{\omega_0}} \cos(\omega_0 t)\sin[(\omega_0+\Delta\omega)\mathrm{t}]dt = \dfrac{2\omega_0(\omega_0+\Delta\omega)\sin\left(\frac{\pi\Delta\omega}{\omega_0}\right)^2}{\Delta\omega\pi(2\omega_0+\Delta\omega)}, \\ LIF(\Delta\omega)_{IM} = \dfrac{2}{T_0}\displaystyle\int_0^{T_0=\frac{2\pi}{\omega_0}} \sin(\omega_0 t)\sin[(\omega_0+\Delta\omega)\mathrm{t}]dt = \dfrac{2{\omega_0}^2\sin\left(\frac{\pi\Delta\omega}{\omega_0}\right)\cos\left(\frac{\pi\Delta\omega}{\omega_0}\right)}{\Delta\omega\pi(2\omega_0+\Delta\omega)}, \\ |LIF(\Delta\omega)| = \sqrt{LIF(\Delta\omega)_{RE}{}^2 + LIF(\Delta\omega)_{IM}{}^2}, \\ when\ \Delta\omega \ll \omega_0, |LIF(\Delta\omega)| \cong \left|\frac{2{\omega_0}^2\sin\left(\frac{\pi\Delta\omega}{\omega_0}\right)\cos\left(\frac{\pi\Delta\omega}{\omega_0}\right)}{\Delta\omega\pi(2\omega_0+\Delta\omega)}\right| \approx \frac{2\omega_0\cos\left(\frac{\pi\Delta\omega}{\omega_0}\right)}{(2\omega_0+\Delta\omega)} \simeq \cos\left(\frac{\pi\Delta\omega}{\omega_0}\right). \end{cases} \quad (1)$$

To measure the frequency independently with high precision, the local frequency spectrum can be fitted to determine the peak frequency, according to the algorithm in the IEEE standard four-parameter sinusoidal fitting method.[22] After further investigation by simulation tests, the three-parameter sinusoidal function $f(x) = \mathbf{A}^* \sin(\mathbf{B}^* x) + \mathbf{C}$ was found to be sufficient to determine the local peak for the target frequency, where x indicates the variant in the local frequency range to be solved with the unit of Hz. As shown in Fig. 2, for a signal with a data length of N = 100 k and a sampling rate of 1000 sps as the detection parameters, the simulated uncertainty for the raw lock-in data at three frequency points is comparable to that at three hundred frequency points, both close to the CRLB for a wide range of SNRs. Notably, during the fitting process, the **A** parameter should be set above zero and the **B** parameter should be properly initialized as $2 * N * T$ to find the target frequency, where N and T represent the data length and time interval, respectively. After the sinusoidal fitting is completed, the measured frequency can be obtained from the optimized parameter $\mathbf{B}_{opt}$ via $\omega_{meas}/2\pi = x_{opt} = (N_{opt} + 0.25)/\mathbf{B}_{opt}$, where N_{opt} is the nearest integer value around $x^*\mathbf{B}_{opt}/2\pi$.

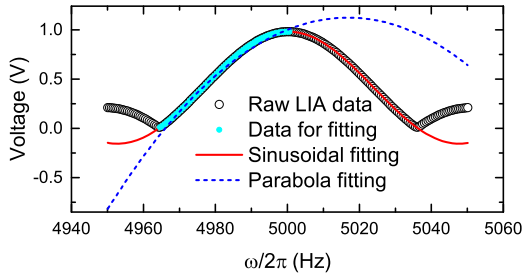

FIG. 1. Principle of the LIF approach.

When analyzing the computational complexity of the LIF method, which is important for applications with large N values, the computational complexity of the fast Fourier transformation (FFT) measured by the number of floating-point operations per second (FLOPS) is proportional to $6N * \log_2(N)$ when N is a power of two and proportional to $6N^2 + 2N(N-1)$ when N is a prime number, as indicated in Ref. 2. The three-point sinusoidal fitting process is N-independent and consumes negligible computer resources, so the computational complexity depends on calculating the amplitudes of three frequency points. The amplitude calculation at each frequency point comes from the root mean square calculation result of the real and imaginary parts. Both the real and imaginary parts for each frequency require N FLOPS, so the entire process costs 6N FLOPS in total, which is $1/\log_2(N)$ times the cost of the FFT.

When the sampling rate is fixed to 1000 sps (corresponding to T = 0.001 s) and the data length is changed from 1000M to 10M,

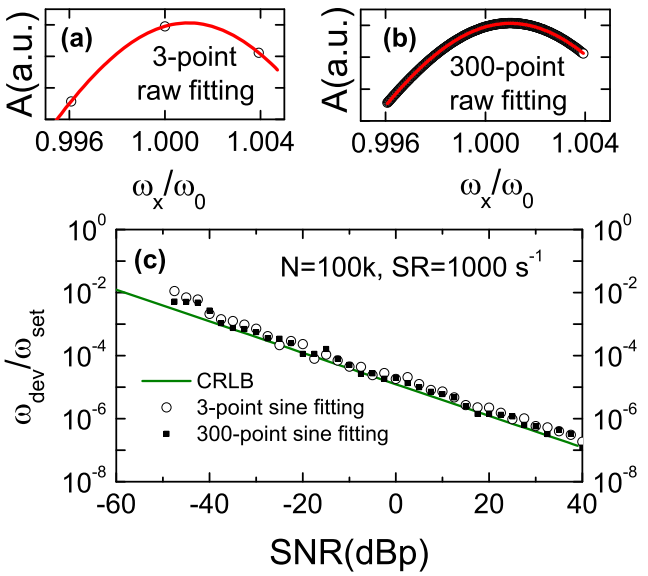

FIG. 2. Dependence of the simulated uncertainty on the number of raw lock-in frequency points. (a) Three-point raw fitting; (b) 300-point raw fitting; (c) comparison of the two fitting processes with the theoretical Cramer–Rao lower bound.

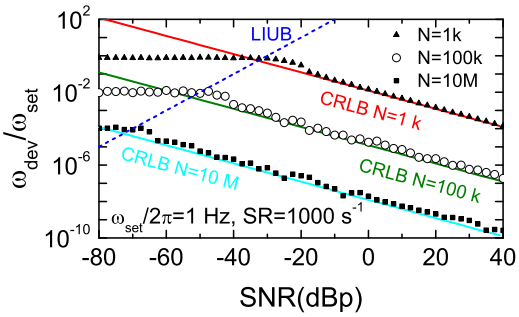

FIG. 3. Comparison of the simulated LIF precision with the theoretical Cramer–Rao lower bound and lock-in upper bound.

as illustrated in Fig. 3, the simulation results indicate that the proposed LIF algorithm is efficient in approaching the CRLB.[13] In addition, the LIF performance is also confined by a lock-in upper bound (LIUB) of the measurement deviation due to the frequency uncertainty caused by white noise. As the dotted lines separate the simulation results in Fig. 3, for each simulation result above the LIUB, there is "saturation" of the measurement deviation below the CRLB, indicating an incorrect working mode of the LIA. The CRLB and LIUB formulas are shown in Eq. (2), where R_p, T, and N denote the SNR in power, time interval, and data length, respectively. In contrast to the CRLB, the LIUB is N-independent and increases rapidly with the increasing SNR, which corresponds to the theoretical resolution of the digital LIA in the frequency range. When the SNR decreases outside the resolution range, the LIF method cannot work in a wider frequency deviation range because the single-bell shape in the local frequency spectrum would be broken by heavy noise,

$$\begin{cases} var(\omega/2\pi)_{LB} \approx \dfrac{6}{(2\pi)^2 R_p T^2 N^3}, \\ var(\omega/2\pi)_{UB} \approx \dfrac{R_p^2}{T^2}. \end{cases} \tag{2}$$

III. IMPLEMENTATION

The proposed LIF algorithm was implemented in a newly designed lock-in device consisting of a front-end amplifier, an ADC acquisition module (18 bits with a 10M sps sampling rate for each channel), an FPGA processing unit, and a liquid-crystal displayer. Figures 4(a) and 4(b) show the implementation structure and the circuit-board appearance of the LIF instrument.

To evaluate the performance of the LIF device, a testing platform was set up, as shown in Fig. 4(c). The LIF testing system includes a signal generator Rigol DG4162, a random noise generator NF WG-721A, an oscilloscope Tektronix DPO4104, and a standard frequency meter Agilent 53132A. DG4162 generates a pure sine wave or mixes uniform white noise for some SNR settings. To produce additional random Gaussian white noise or pink noise, the output of DG4162 was connected to the input of WG-721A, which can generate random noise in a finely tunable manner and output signals and noise for testing with various SNR settings. The accuracy and precision of the mixed signals are then tested by the LIF instrument and 53132A, as shown in Fig. 4. DPO4104 is used when checking or recording waveforms for further analysis.

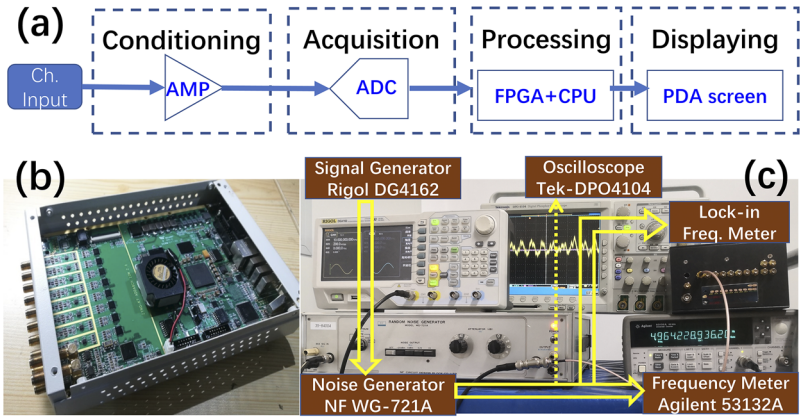

FIG. 4. (a) Implementation structure and (b) circuit-board of the LIF device. (c) Testing platform with a signal generator, a noise generator, and a standard frequency meter as well as the LIF instrument, where an oscilloscope is used for recording raw waveforms when necessary.

To be systematic in the investigation, the LIF instrument was tested for its dependence on the SNR, frequency, amplitude, noise types, and time. The time constant of the LIF method was fixed at 1 s in this work, and equivalently, the gate time of the 53132A frequency meter was also fixed at 1 s. Except for the time-dependent tests, the number of tests was taken as 100 for all combined factors of the SNR, frequency, amplitude, and noise types to be statistically meaningful. Both 53132A and the LIF instrument produce frequency measurement results $\omega_{meas}/2\pi$, which then generate a mean frequency $\omega_{mean}/2\pi$ and a standard deviation $\omega_{dev}/2\pi$, with a unit of Hz. In addition, the LIF instrument can output the amplitude of the measured frequency and the corresponding phase difference. For a single channel signal, the phase difference cannot be used, so it is omitted when discussing the results of the current work. Using the same statistical analysis, amplitude measurements generate a mean amplitude $V_{p\text{-}mean}$ and a standard deviation $V_{p\text{-}dev}$.

IV. DISCUSSION

The SNR-dependent frequency measurement is shown in Fig. 5. It is found that the accuracy of the 53132A frequency meter gradually decreases when the SNRs of the Gaussian white noise mixed signals decrease below 10 dBp (10 dB in power), while the LIF instrument can correctly work even when the SNRs are as low as −40 dBp, with $\omega_{dev}/\omega_{mean} < 1 \times 10^{-5}$ relative deviations, which are comparable to the theoretical CRLB simulation results shown in Fig. 3 (the N = 10M CRLB line reads a 1.2×10^{-6} relative deviation at an SNR of −40 dBp).

Figure 6 shows the frequency-dependent result of the LIF instrument. To compare the accuracy and precision of the instrument with those of a standard frequency meter, pure sine waves with an amplitude of 0.2 V were generated by DG4162, which has a resolution of 1 μHz. The relative deviation of the LIF instrument approaches 1×10^{-9} around 10 kHz, corresponding to an absolute precision of 10 μHz at 10 kHz. At lower frequencies, the uncertainty is higher because for a finite time constant (TC = 1 s in this work), the periods for measurement are limited, while at higher frequencies, the higher uncertainty is due to the finite sampling rate of the LIF instrument.

Aside from the high precision frequency measurements, the LIF instrument can measure the amplitude of signals at the determined frequency point with reasonable precision. As shown in Fig. S7 and Table I in the supplementary material, at lower SNRs down to −40 dBp, the LIF instrument correctly measured the frequency and amplitude at the same time with high precision, and the noise type dependence of accuracy was not found. Three kinds of noise were investigated in this work: Gaussian white noise, Gaussian pink noise, and uniform white noise. It is worth mentioning that the

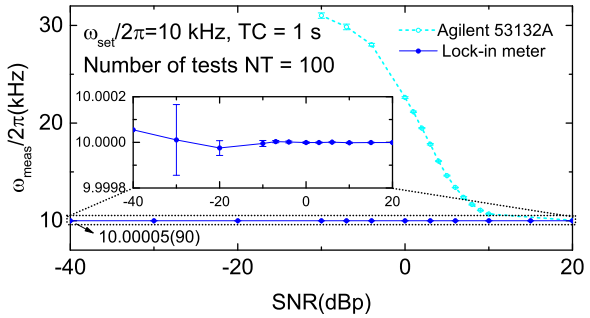

FIG. 5. Frequency measurement results for real Gaussian white noise mixed signals of different SNRs compared to results from the Agilent 53132A frequency meter.

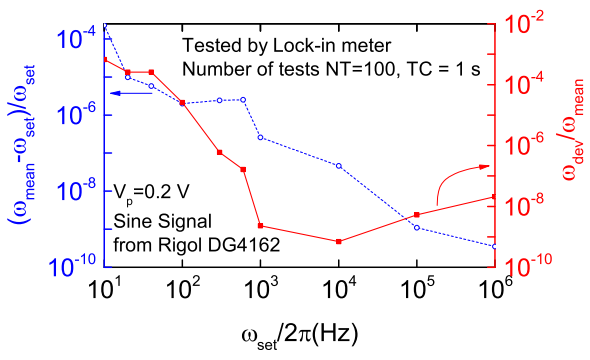

FIG. 6. Frequency-dependent LIF measurement results.

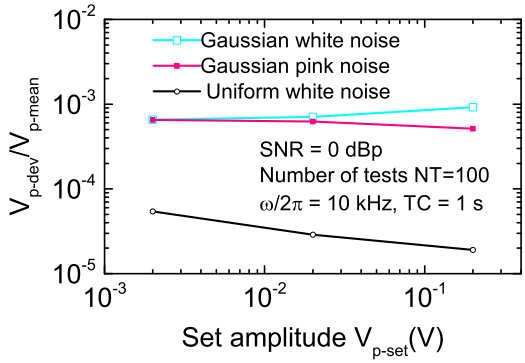

FIG. 7. Amplitude-dependent LIF measurement results for signals with Gaussian white noise, Gaussian pink noise, and uniform white noise at a fixed SNR of 0 dBp.

noise type influences the precision of the amplitude measurement. Figure 7 shows that uniform white noise has the least deviation, which is obviously because uniform white noise has a lower fixed peak value. Gaussian random white noise and pink noise have slight differences even when the noise power and SNR are equal, which is understandable because the Gaussian distribution of white noise is broader than that of pink noise for a fixed noise power. As a result, Gaussian white noise has a higher peak value and thus causes larger deviations.

It is useful to test the time-dependent behavior of real applications. Taking 10 kHz as an example, repeated measurements have been recorded, as shown in Fig. 8(a), where the statistically relative accuracy and precision are approximately 5×10^{-9} and 7×10^{-11}, respectively. The precision is much higher than that shown in Fig. 5 simply because the noise generator was turned off and only a pure sinusoidal wave was tested. To ensure that each measurement was

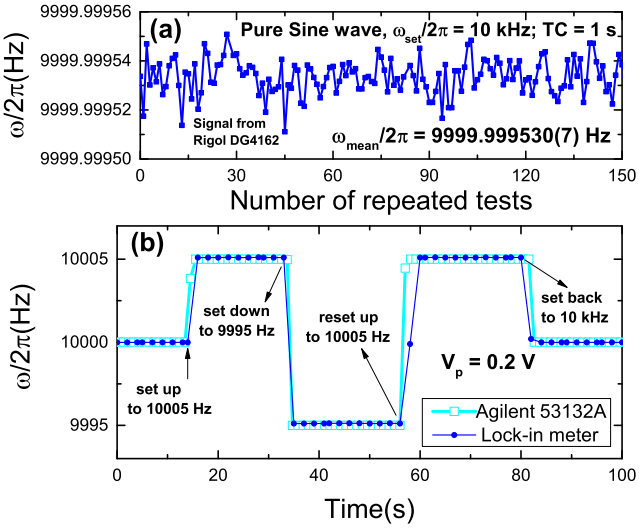

FIG. 8. (a) Repeated LIF test results for pure sine signals at 10 kHz and (b) a comparison of response time tests to the results of a standard frequency meter.

independent in the set time constant of 1 s, the set frequencies were flipped upward and downward several times, and the result in Fig. 8(b) shows no obvious delay outside of the set time constant, in high consistence with the standard frequency meter.

Therefore, the LIF method can measure both frequency and amplitude with high precision and efficiency. Nevertheless, this does not mean that the LIF method will completely replace normal FFT-like methods because the LIF method struggles to measure frequencies over a wide frequency range and prior knowledge of the local frequency is necessary. As a result, the LIF method is best suited for the determination of finite frequencies that drift slowly over a small frequency range.

V. CONCLUSION

In this paper, we have proposed a novel LIF method for frequency measurements based on innovations in both frequency measurements and LIA techniques. The local frequency spectrum of the sinusoidal function is shown to be better than that of the parabola function. Furthermore, simulation results demonstrate that the LIF results have a standard deviation approaching the CRLB with an N-proportional computational complexity, which is obviously better than that of the FFT method, which is $N * \log_2(N)$-dependent. The implemented LIF instrument can perform both frequency measurements and amplitude measurements at the same time, even when the SNRs are significantly low. As a complement to classic frequency measurement techniques, which can perform wide frequency measurements, the LIF method provides a new possibility for local fine frequency measurements.

SUPPLEMENTARY MATERIAL

See the supplementary material for the LIF simulation programs (coded in the Labview platform) and detailed LIF testing information, including Figs. S1–S8 and Tables S1 and S2.

ACKNOWLEDGMENTS

This work was supported by the National Natural Science Foundation of China (Grant No. 51327806), the Fujian Institute of Innovation (Grant No. FJCXY18040302), and the Youth Innovation Promotion Association of the Chinese Academy of Sciences (Grant No. 2018009). The author thanks Mr. Xiaoshou Dai and Chunsheng Xiong from the Yanchuangda Company for their help in realizing the LIF instrument into the FPGA, Mr. Shichao Zhou for his assistance during LIF testing, and Professor Ling-An Wu for useful discussions.

DATA AVAILABILITY

The data that support the findings of this study are available from the corresponding author upon reasonable request. The data that support the findings of this study are available within the article (and its supplementary material).

REFERENCES

[1] Metrological Editorial Committee, *Metrological Testing Technical Manual Volume 11: Time and Frequency* (China Metrology Press, Beijing, 1996).
[2] T.-H. Li, *Time Series with Mixed Spectra* (CRC Press, London, 2016); A. V. Oppenheim and R. W. Schafer, *Discrete-Time Signal Processing* (Pearson Education, London, 2010).
[3] K. Hofbauer, "Estimating frequency and amplitude of sinusoids in harmonic signals: A survey and the use of shifted Fourier transforms," Diploma thesis, Graz University of Technology, Austria, 2004.
[4] S. Zhou and Z. Shancong, Circuits Syst. Signal Process. **37**, 5680 (2018).
[5] S. Tretter, IEEE Trans. Inf. Theory **31**, 832 (1985).
[6] C. Candan, IEEE Signal Process. Lett. **20**, 913 (2013).
[7] E. Jacobsen and P. Kootsookos, IEEE Signal Process. Mag. **24**, 123 (2007).
[8] B. G. Quinn, IEEE Trans. Signal Process. **42**, 1264 (1994).
[9] T. Grandke, IEEE Trans. Instrum. Meas. **32**, 350 (1983).
[10] E. Aboutanios and B. Mulgrew, IEEE Trans. Signal Process. **53**, 1237 (2005).
[11] B. Boashash, Proc. IEEE **80**, 540 (1992).
[12] E. Jacobsen, On local interpolation of DFT outputs, http://www.ericjacobsen.org/FTinterp.pdf, 2002.
[13] D. Rife and R. Boorstyn, IEEE Trans. Inf. Theory **20**, 591 (1974).
[14] D. C. Rife and R. R. Boorstyn, Bell Syst. Tech. J. **55**, 1389 (1976).
[15] E. Nitzan, T. Routtenberg, and J. Tabrikian, IEEE Trans. Signal Process. **67**, 753 (2019).
[16] D. Belega and D. Petri, Signal Process. **117**, 115 (2015).
[17] X. Huang, J. Xu, and Z. Wang, Sensors **18**, 4334 (2018).
[18] L. N. Kazakov, I. V. Luk'yanov, and B. I. Shakhtarin, J. Commun. Technol. Electron. **63**, 805 (2018).
[19] A. Serbes, in *International Telecommunications Conference* (Springer, 2019), p. 281.
[20] N. Y. Bey, Signal Image Video Process. **12**, 1279 (2018).
[21] M. L. Meade, *Lock-In Amplifiers: Principles and Applications* (Peter Peregrinus, London, 1983).
[22] IEEE, *IEEE Std 1057-2007 for Digitizing Waveform Recorders* (IEEE, New York, 2008).

Supplementary materials for “Lock-in frequency measurement with high precision and efficiency”

Jun LU (陆俊)

E-mail: lujun@iphy.ac.cn

Institute of Physics, Chinese Academy of Sciences/Beijing National Laboratory for Condensed Matter Physics, Beijing 100190, China

A1. Notes for LIF simulation programs

Programs are uploaded and free for download: https://github.com/iop-lujun/LIF .

To clarify the principle and process of the new frequency meter based on the digital lock-in algorithm introduced in the main text, the author has decided to release the related simulation programs, which have been developed and maintained in Labview for more than ten years (the author released his digital lock-in source codes when publishing the first paper about virtual lock-in amplifiers in 2008 when he was a PhD student , see https://doi.org/10.1088/0957-0233/19/4/045702). The FPGA source C codes are unfortunately held by a collaborator, which the current author has no permission to release, but the Labview version is quite sufficient to understand and realize the lock-in frequency meter (LIF) proposed by the current author.

Because the Labview programming environment is user friendly, one could easily handle the source codes with some fundamental practice on Labview. After opening the entry file “3G-LIA test simulator 2020.vi”, the front panel of the LIF simulation program appears as in Fig. S1. Although the hierarchical structure of the package is rather comprehensive, as shown in Fig. S2, the necessary code files developed by the current author are not in the “SimLIF2020.LLB” package, as shown in Fig. S3, which could be opened by NI Labview LLB manager with a version later than 2016.

The simulation programs have been coded in English and can generate Gaussian white noise and mixed signals with set SNRs, perform LIF calculations, and obtain frequency,

amplitude, phase difference, and SNR values.

Permission is hereby granted, free of charge, to any person obtaining a copy of this software and the associated documentation files (the "Software") to use the Software without restriction, including without limitation of the rights to use, copy, modify, merge, publish, distribute, sublicense, and/or sell copies of the Software, and to permit persons to whom the Software is furnished to do so, subject to the conditions of citing or referring to the current article titled “Lock-in frequency measurement with high precision and efficiency”. Feedback information to improve the LIF simulation software is welcome and should be submitted to the current author using the corresponding email address.

THE SOFTWARE IS PROVIDED "AS IS", WITHOUT WARRANTY OF ANY KIND, EXPRESS OR IMPLIED, INCLUDING BUT NOT LIMITED TO THE WARRANTIES OF MERCHANTABILITY, FITNESS FOR A PARTICULAR PURPOSE, AND NONINFRINGEMENT. IN NO EVENT SHALL THE AUTHOR BE LIABLE FOR ANY CLAIM, DAMAGES, OR OTHER LIABILITY, WHETHER IN AN ACTION OF CONTRACT, TORT, OR OTHERWISE, ARISING FROM, OUT OF, OR IN CONNECTION WITH THE SOFTWARE OR THE USE OR OTHER DEALINGS IN THE SOFTWARE.

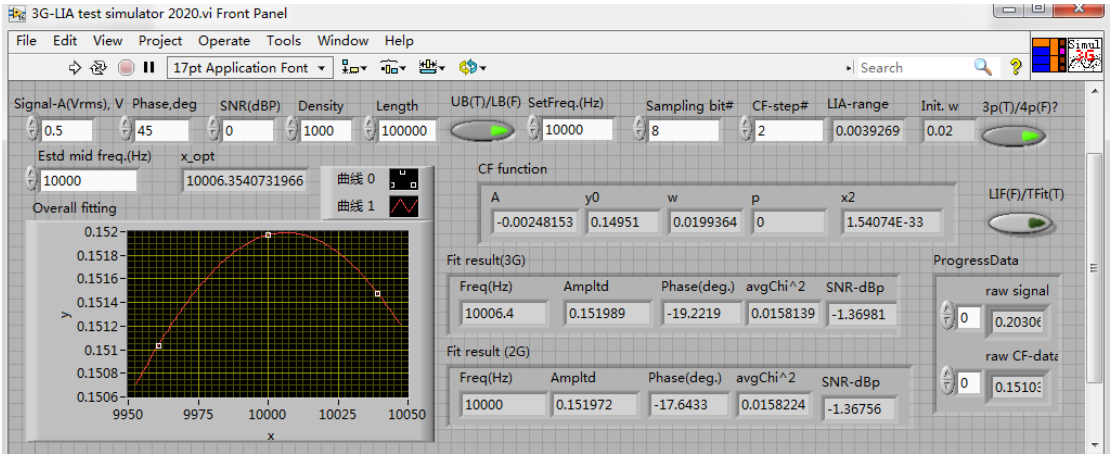

Fig. S1. User interface of the LIF simulation Labview program distributed by the current author.

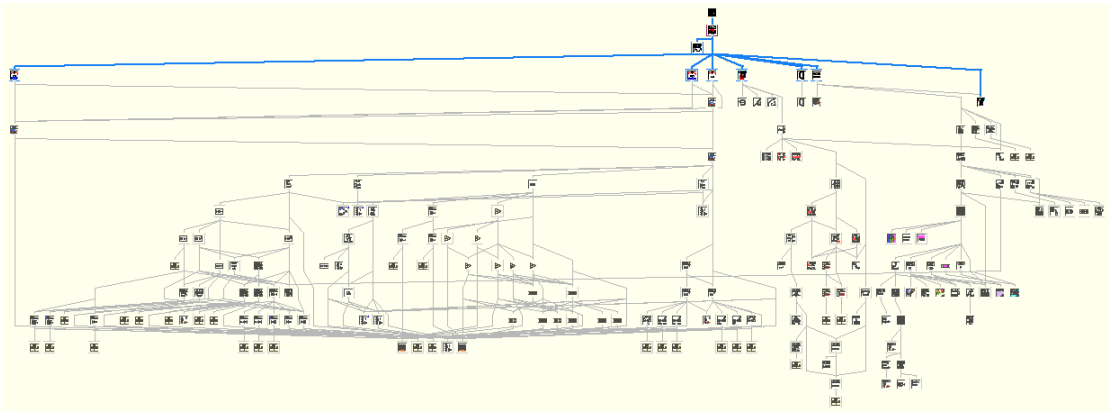

Fig. S2. The hierarchical structure of the LIF simulation program.

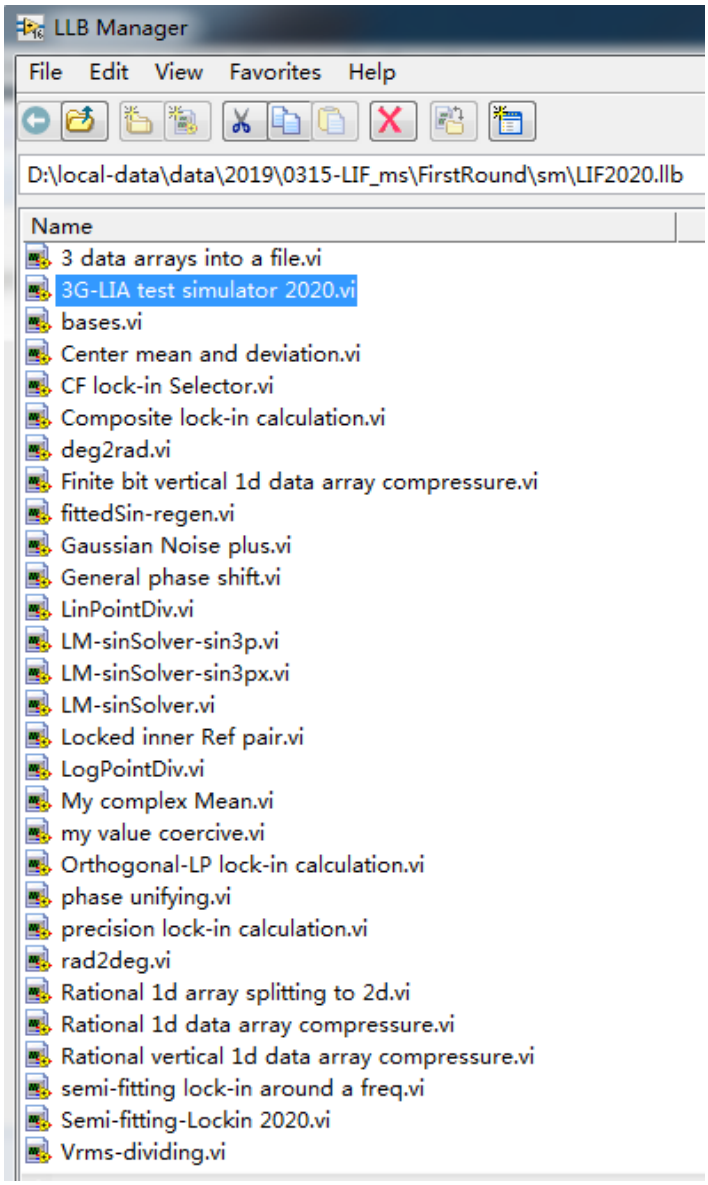

Fig. S3. Content of the distributed LIF simulation package programmed by the current author.

A2. Detailed LIF testing information

As shown in Fig. 5 in the main text, the LIF testing platform includes a Rigol DG4162 signal generator, an NF WG-721A random noise generator, an oscilloscope, and an Agilent 53132A standard frequency meter. The accuracy and precision of the signal generator have been evaluated by firstly using the 53132A frequency meter, as shown in Fig. S4. The random noises generated from the NF WG-721A are analyzed after recording the waveforms with the Tektronics DPO4104 oscilloscope. The results are shown in Fig. S5, where both white and pink noise are Gaussian-distributed, and the maximum bandwidth is approximately 50 kHz, as specified by NF company. From the performances of the signal generator and the random noise generator, the main frequency used in the main text has been chosen at 10 kHz. It

should be noted that the NF WG-721A cannot produce uniform noise, but the DG4162 does produce a signal with mixed uniform noise when properly configured. As a result, three types of noise in total have been investigated in this work.

To support the SNR-dependent measurements used in the main text, the raw waveforms with typical SNRs have been recorded by the DPO 4104, as shown in Fig. S6, and calculated by the program introduced in section A1.

In the main text, when discussing the amplitude-dependent LIF method, only the precision is comprised of Gaussian white noise, Gaussian pink noise, and uniform noise because the accuracy is almost the same for the three types of noise, as shown in Fig. S7.

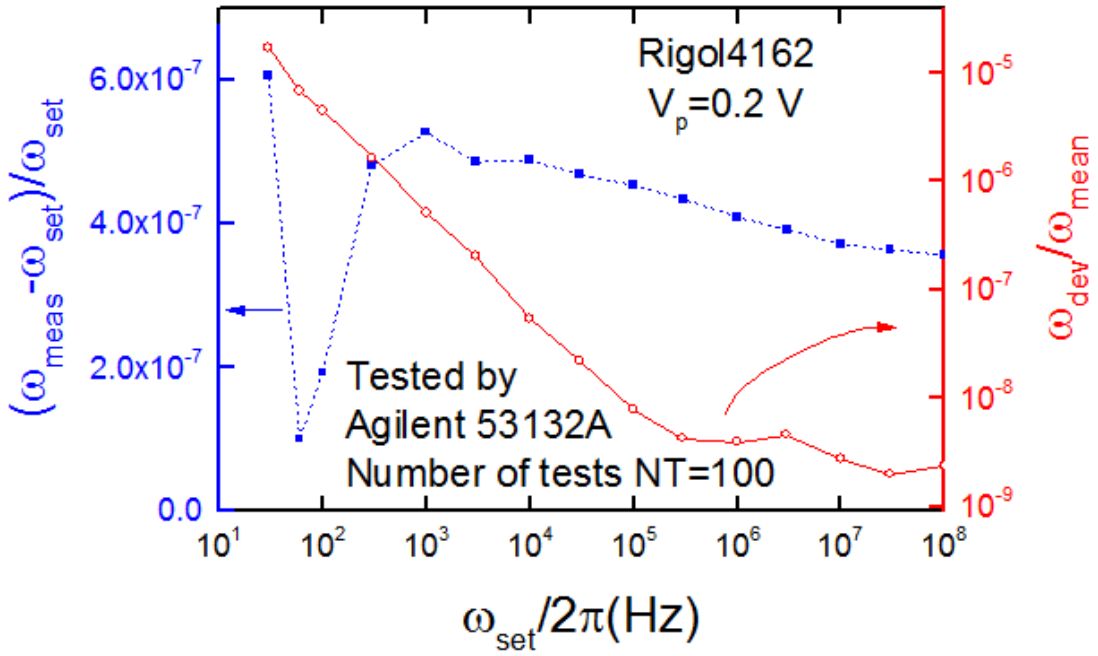

Fig. S4. Frequency dependence of the accuracy and precision of the pure sine wave generated by the Rigol DG4162 and measured by the Agilent 53132A, with an amplitude of 0.2 V.

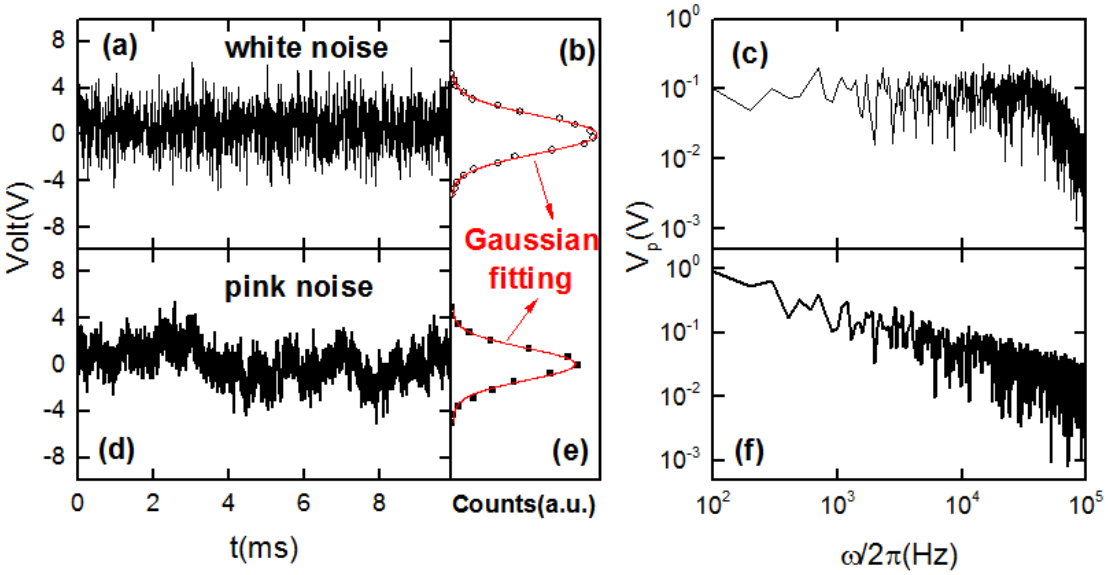

Fig. S5. Two types of random noise generated from the NF WG-721A, where (a) and (d) are the waveforms of white noise and pink noise, respectively; (b) and (e) are the histograms of

(a) and (d), respectively; and (c) and (f) are the frequency spectra of (a) and (d), respectively.

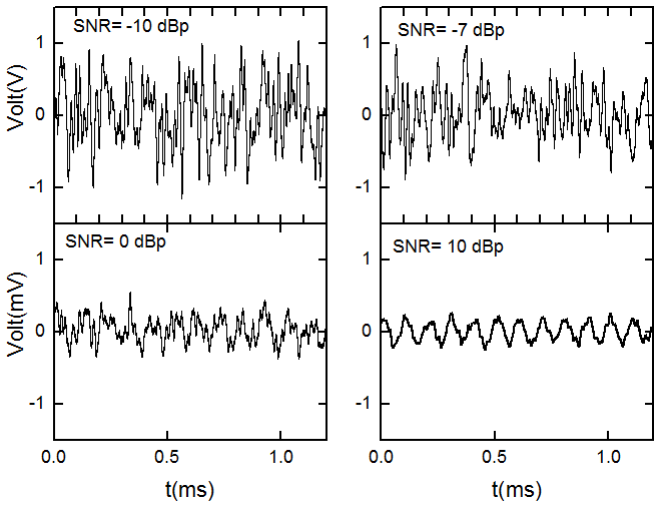

Fig. S6. Demonstration of waveforms with different signal-to-noise ratios (SNRs), where the amplitude of the disturbed sine signal is Vp=0.2 V, and the noise type is Gaussian white noise.

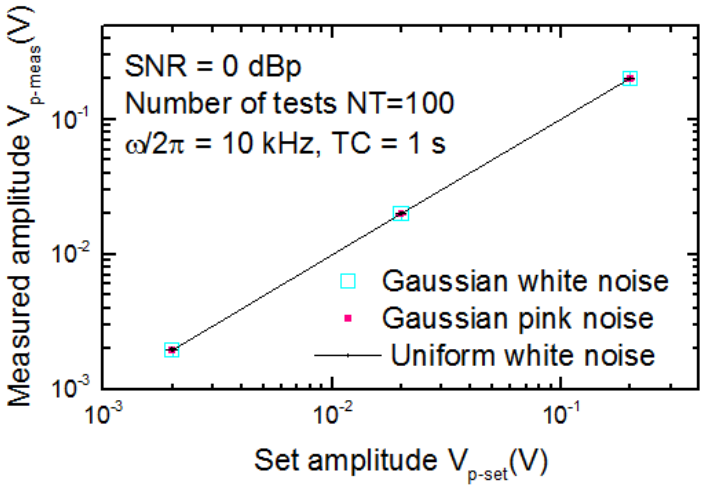

Fig. S7. Demonstration of the accuracy of the LIF method, where the measured objects have an SNR= 0 dBP with different types of noise.

A3. Datasheets of main LIF testing results

Table S1. Raw data of Fig. 6 in the main text, where LIF denotes lock-in frequency meter, AgF denotes the Agilent 53132A frequency meter, all noise types are Gaussian random white noise generated by the NF WG-721A, and the unit of ω/2π is Hz.

SNR (dBP)	Mean of ω/2π (Measured by LIF)	Deviation of ω/2π (Measured by LIF)	Set Vp (V)	Mean of Vp (Measured by LIF)	Deviation of Vp (Measured by LIF)	SNR (dBP)	Mean of ω/2π (Measured by AgF)	Deviation of ω/2π (Measured by AgF)
-60	9987.688	2.61E+00	2.00E-04	4.06E-04	5.57E-04	-10	31020.38	278.37
-50	9991.172	6.68E+00	2.00E-03	1.59E-03	1.58E-03	-7	29855.01	280.63
-40	10000.05	1.01E+00	2.00E-03	1.65E-03	4.48E-04	-4	28036.54	131.84
-30	10000.01	1.55E-01	2.00E-02	1.93E-02	8.90E-04	0	22628.28	84.86
-20	9999.975	3.25E-02	2.00E-02	1.98E-02	1.05E-04	1	21164.4	65.41
-10	9999.995	1.30E-02	2.00E-01	2.00E-01	3.89E-04	2	19496.11	60.15
-7	10000	4.84E-03	2.00E-01	2.01E-01	3.83E-04	3	17833.86	76.52
-4	10000	4.14E-03	2.00E-01	2.00E-01	2.63E-04	4	16109.99	54.94
0	9999.999	3.70E-03	2.00E-01	2.00E-01	1.18E-04	6	13409.93	35.41
3	9999.999	2.40E-03	2.00E-01	2.00E-01	1.10E-04	7	12407.26	76.95
6	10000	2.17E-03	2.00E-01	2.00E-01	8.56E-05	8	11665.13	43.86
10	9999.998	2.66E-03	2.00E-01	2.00E-01	8.21E-05	9	11072.94	29.77
15	9999.999	1.50E-03	2.00E-01	2.00E-01	4.09E-05	10	10702.16	31.45
20	10000	4.59E-04	2.00E-01	2.00E-01	1.31E-05	20	10043.19	10.98

Table S2. Raw data of Fig. 8 in the main text, where the unit of ω/2π is Hz.

Noise types	Mean of ω/2π (Measured by LIF)	Deviation of ω/2π (Measured by LIF)	Set Vp (V)	Mean of Vp (Measured by LIF)	Deviation of Vp (Measured by LIF)
Gaussian white noise	10000.0013	3.38E-03	2.00E-01	2.00E-01	1.81E-04
	9999.9991	3.07E-03	2.00E-02	1.99E-02	1.41E-05
	9999.9995	3.44E-03	2.00E-03	1.94E-03	1.26E-06
Gaussian pink noise	10000.0008	3.02E-03	2.00E-01	2.00E-01	1.07E-04
	10000.0010	2.66E-03	2.00E-02	1.99E-02	1.24E-05
	10000.0002	3.13E-03	2.00E-03	1.94E-03	1.26E-06
Uniform white noise	9999.9995	6.85E-06	2.00E-01	2.01E-01	4.11E-06
	9999.9995	2.23E-05	2.00E-02	2.00E-02	7.84E-07
	9999.9995	9.46E-05	2.00E-03	1.96E-03	1.20E-07

A4. Accuracy analysis of the LIF method

The accuracy of the LIF method is obviously dependent on the proximity of the initial frequency. To what extent does the proximity influence the accuracy? In principle, the range of the initial frequency should be below $W_{double\text{-}side}$(Hz)=1/TL/10^(SNR/20), where TL is the time length of testing with the unit of seconds, and SNR is the signal-to-noise ratio with a unit of dBp. A frequency-difference-dependent simulation was performed, and the result is shown in Fig. S8, where the test frequency is 1 Hz, and the sampling time is 100 s. When the relative difference of the initial value is larger than 0.2%, the accuracy decreases up to 400 ppm from statistical precision. Quantitative analysis of such a turning point requires further mathematical investigation, but confining the initial frequency difference below 1/5/TL/10^(SNR/20) is suggested for practical purposes to obtain a high accuracy.

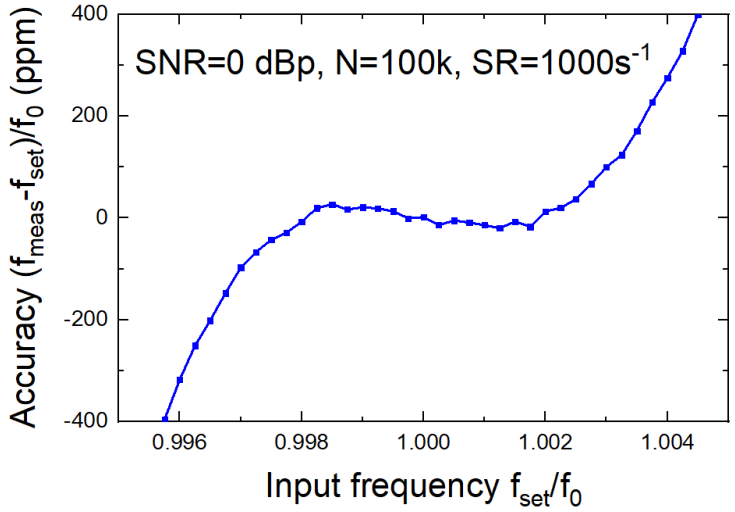

Fig. S8 Simulated LIF accuracy for a 0 dBp signal plus Gaussian white noise.